Block Copolymer Supramolecular Assembly beyond Hydrogen Bonding

ARTICLE *in* MACROMOLECULES · DECEMBER 2011

Impact Factor: 5.8 · DOI: 10.1021/ma2011798

3 AUTHORS, INCLUDING:

Alexander Sidorenko
University of the Sciences in Philadelphia
53 PUBLICATIONS **2,083** CITATIONS

Macromolecules

Article

pubs.acs.org/Macromolecules

Block Copolymer Supramolecular Assembly beyond Hydrogen Bonding

Daniel Hagaman, Timothy P. Enright, and Alexander Sidorenko*

Department of Chemistry & Biochemistry, University of the Sciences, Philadelphia, Pennsylvania 19104, United States

Supporting Information

ABSTRACT: Supramolecular assemblies of block copolymers (BSAs) with low molecular weight additives require preferential interactions between the additive and one of the blocks. So far, only hydrogen bonds (HB) were explored to obtain BSAs. We report on three novel BSAs of block copolymer PS-*block*-P4VP with commercially valuable additives of the EDOT family. Two of the additives ((3,4-ethylenedioxythiophene) (EDOT) and 3,4-(2,2-dimethylpropylenedioxy)thiophene (ProDOT)) form the BSAs based on interactions others than HB. The morphology and some properties of the BSAs were studied by means of AFM, FTIR, and spectroscopic ellipsometry. The BSAs reveal cylindrical morphology with periodicity of ~30 nm. In thin films the orientation of the cylinders can be switched from perpendicular to parallel by annealing in vapors of a suitable solvent. Extraction with a selective solvent results in porous films with porosity of ~15%. These non-HB BSAs were compared with the HB BSA of HMeDOT as well as HABA BSA reported recently. The nature of the non-HB interactions is briefly discussed.

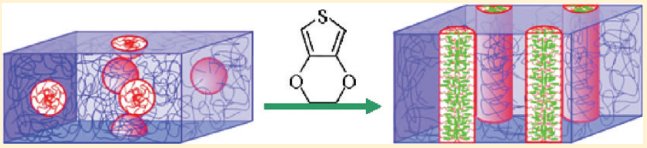

INTRODUCTION

The phenomenon of microphase separation in block copolymers (BCP) is a classic example and illustration of self-assembly in complex systems. A single molecule of BCP contains two or more different polymer chains, or blocks, connected by a covalent bond. The covalent linkage between immiscible blocks defeats macrophase separation caused by the entropy of mixing of polymer blends.[1,2] As a result, the blocks of one type segregate into domains with dimensions between 5 and 100 nm and several specific patterns. In the simplest case of diblock copolymers the gradual increase of volume fraction of one of the blocksproduces the following evolution of morphologies: body-centered spheres, hexagonally packed cylinders, bicontinuous double gyroid, and lamellae, with the same pattern repeating in inverse order.[1,3]

Ikkala et al.[4,5] have developed a new class of metamaterials, i.e., block copolymer supramolecular assemblies (BSA). One of the blocks of a BCP is selectively modified by a hydrogen-bonded additive of low molecular mass. The classic example is poly(styrene-*block*-4-vinylpyridine), PS-*block*-P4VP, with *n*-pentadecylphenol (PDP) reversibly attached to the P4VP block by H-bond formed between the nitrogen of pyridine and the hydroxyl group of PDP. Other examples include octyl gallate,[6,7] 1,5-dihydroxynaphthalene,[8] 2-(4′-hydroxybenzeneazo)-benzoic acid (HABA),[9,10] azo-dye DR1,[11] 1-pyrenebutyric acid,[12] quaterthiophene,[13] resorcinol,[14] carbohydrates,[15] dodecylbenzenesulfonic acid,[16] and bent-core additives.[17] Several special cases describe self-assembly in BSAs of triblock copolymers[18] and H-bonded carboxylthiophene attached to side-chain pyridine-terminated dendrimers.[19]

It is worth to define in greater detail the term "block copolymer supramolecular assembly". It is used to define the system of a block copolymer and a low molecular weight additive formed via selective noncovalent interactions between the additive and one of the blocks of the parent BCP. We use this term to distinguish our system from supramolecular assemblies of small molecules as well as mixtures of block copolymers and homopolymers recently developed by Russell et al.[20] The term itself and the abbreviation BSA stress the dualistic nature of the system: polymer basis (block copolymer) and small molecules (supramolecular) as an additive to form the entire system (assembly).

The presence of a weakly attached additive in one of the domains can qualitatively alter its morphology and properties. First, the morphology changes occur due to bulky additives selectively associated with one of the blocks. Second, BSAs eventually reveal hierarchical "structure-within-structure" morphologies due to smaller length-scale organization of additives (e.g., PDP) within one of the domains (P4VP + PDP).[21] Moreover, because of the high mobility of H-bonded molecules of the additive, the microphase separation in BSAs occurs quicker and can result in better ordering compared to neat BCPs. Third, a universal and practically valuable feature of BSAs is a possibility to extract the additive from the BSA bulk or film. Being attached by weak H-bonds, they can be easily removed by selective solvents, leaving nanoporous materials.[4,9] The latter can be used as nanotemplates for sol–gel reaction,[22] metal decoration,[23−25] and reactive deposition of metal nanoparticles[9,10] and polyaniline.[26]

Self-assembly in thin films of BSA is of particular interest and challenge. The presence of a distinguishing dimension, i.e.,

Received: May 24, 2011
Revised: November 1, 2011
Published: December 12, 2011

height as opposed to lateral dimensions, allows us to consider orientation of cylinders and lamellae as perpendicular or parallel to the substrate surface plane. Two interfaces—free surface (air−BSA) and substrate−BSA interface—play a critical role in pattern formation. The effect of preferential interaction of one or more blocks with the interfaces in many cases makes the parallel orientation of BCP in thin films more favorable.[27] In the context of this article it is worth to mention the phenomenon of terrace formation which is typically observed in the case of parallel oriented domains, both cylinders and lamellae.[9,10,28] The thickness of the BSA films is another important factor that governs thermodynamics of the layers. Ideally, the domains confined between two interfaces will either form the terraces or adopt the perpendicular orientation.[29] The additive can significantly modify the BSA morphology if it preferentially occupies either surface of the film.[8−10,28,30]

The unique properties of BSAs originate from mobile additives attached by reversible hydrogen bonds (HB)[31] and other weak interactions including Coulombic and solvophobic ones.[32] In order to extend the range of available additives, other weak interactions can be explored as well. In this paper we test the hypothesis that non-HB interactions can serve as a basis to form the BSA instead of HB. We have chosen PS-*block*-P4VP as a parent BCP. Being potentially rich in different intermolecular interactions (HB, π-stacking, dipole−dipole, donor−acceptor), the block of P4VP is a very promising model for our needs. The choice of the counterpart (low molecular weight additive) is based on possible complementarities to P4VP and prospective applications. Taking into account the growing commercial importance of (3,4-ethylenedioxythiophene) (EDOT) as a precursor for the electroconductive polymer PEDOT,[33,34] our natural choice was EDOT and the family of commercially available EDOT-like compounds. The two dioxythiophene derivatives, namely 3,4-(2,2-dimethylpropylenedioxy)thiophene (ProDOT) and hydroxymethyl-3,4-ethylenedioxythiophene (HMeDOT), were used as the additives to form either the HB BSA (HMeDOT) or the non-HB BSA (EDOT, ProDOT) (Figure 1).[35−38] In both cases we assumed selective interactions

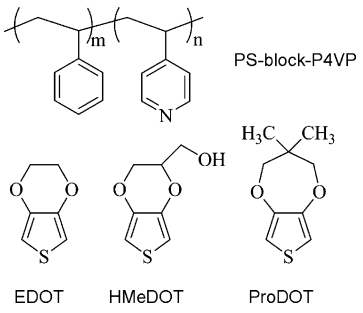

Figure 1. Parent BCP and the low molecular weight additives of the EDOT family: (3,4-ethylenedioxythiophene) (EDOT), 3,4-(2,2-dimethylpropylenedioxy)thiophene (ProDOT), and hydroxymethyl-3,4-ethylenedioxythiophene (HMeDOT) used in this work as the model compounds.

between the additive and the 4-vinylpyridine units of the of the parent BCP.

RESULTS

FTIR Spectroscopy. We begin our discussion with the analysis of the FTIR spectra of the BSAs and the corresponding low molecular weight additives. The survey FTIR spectra of an equimolar (with respect to P4VP content) compositions with ProDOT and HMeDOT are shown in the Figure 2a.

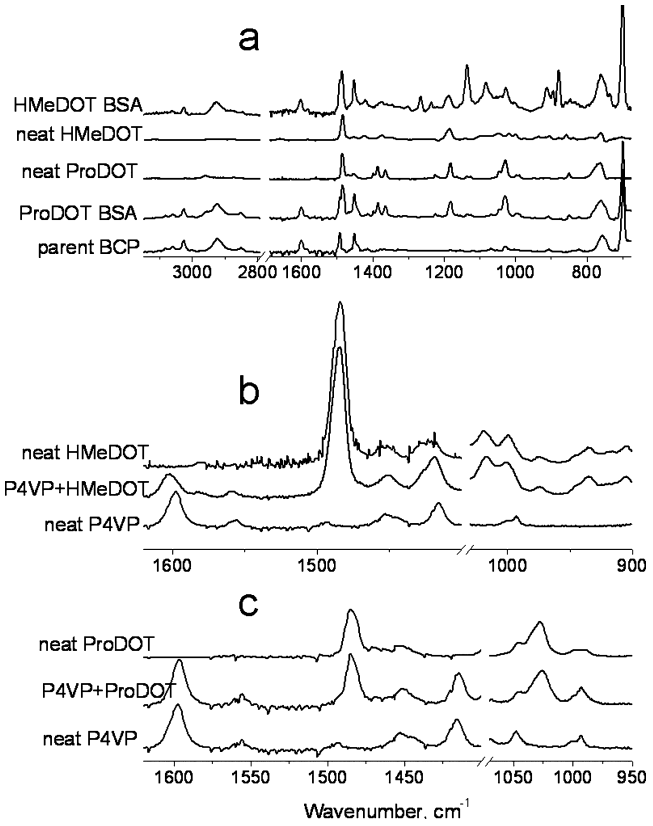

Figure 2. FTIR (ATR) spectra of neat HMeDOT, neat ProDOT, and corresponding BSAs with the parent BCP (survey spectra, a), HMeDOT associated with P4VP homopolymer (b), and ProDOT associated with P4VP (c).

The spectra were obtained from films of the compositions deposited by drop-casting with an ATR accessory. Both compositions formed homogeneous films with no signs of the macrophase separation of the additives. This provides evidence for the formation of some kind of molecular association of both additives with the BCP.[39] In the case of HMeDOT we anticipated the formation of a hydrogen bond between −OH group of the additive and the pyridine ring of the P4VP block.

On the basis of previous publications[40−43] and their own previous experiments, Ikkala et al.[5] identified three absorption bands of P4VP affected by HB formation, i.e., 1597, 1415, and 993 cm^{-1}. In spite of our expectations, we were not able to observe shifts in the pyridine ring absorption bands. The same observations were made for ProDOT. The detailed consideration of the spectra showed that the P4VP peak at 1597 cm^{-1} was masked by the overlapping PS peak at 1600 cm^{-1} (and PS constitutes the vast majority of the composition). Also, the peaks at 1415 and 993 cm^{-1}, being weak themselves, are complicated by the peaks of the additives. Apparently, the presence of the PS block makes further analysis unreliable. Therefore, we have performed more detailed analysis using two model systems: comblike homopolymers of P4VP/HMeDOT (Figure 2b) and P4VP/ProDOT (Figure 2c). (Here we adopt the terminology used by Ikkala and other researchers to refer to the homopolymers with side-chain additives attached by weak interactions, i.e., HB as opposed to comb-shaped polymers

dx.doi.org/10.1021/ma2011798 | *Macromolecules* 2012, 45, 275−282

carrying covalently attached mesogenic side groups according to ref 44.)

Similarly to previously reported examples with phenols, amines, alcohols, and carboxy acids,[5,45] formation of a HB with P4VP results in a significant shift of the IR absorption bands responsible for the pyridine ring vibrations. As shown in the Figure 2b, hydrogen bonding with HMeDOT results in a shift of the bands. Being the least screened out, the peak at 1597 cm^{-1} reveals a clear shift to 1604 cm^{-1}. Also, the peak at 1415 cm^{-1} shifts to 1419 cm^{-1}. The peak around 1000 cm^{-1} overlaps with the two IR bands of HMeDOT as well as ProDOT. However, the detailed analysis reveals the shift of the pyridine peak from 993 to 1009 cm^{-1} in the HMeDOT BSA (see Supporting Information). These shifts clearly indicate the formation of a HB between HMeDOT and the P4VP units. On the contrary, ProDOT assembly shows no shifts in the characteristic IR absorption bands of the P4VP block (Figure 2c). This observation proves our *a priori* assumption based on the absence of polar group; i.e., ProDOT cannot form HB with P4VP.

Spectroscopic ellipsometry was routinely used as a method of film thickness measurements together with the AFM scratch test. Besides that, we used both methods for analysis of the porosity of the films upon extraction of the additives (HMeDOT and ProDOT) by methanol. Being associated with P4VP blocks either by HB or non-HB interactions, we assumed that the additives can be easily removed by selective solvent, i.e., methanol. Indeed, ellipsometry demonstrated a significant shift in both Ψ (Figure 3) and Δ spectra of HMeDOT and ProDOT

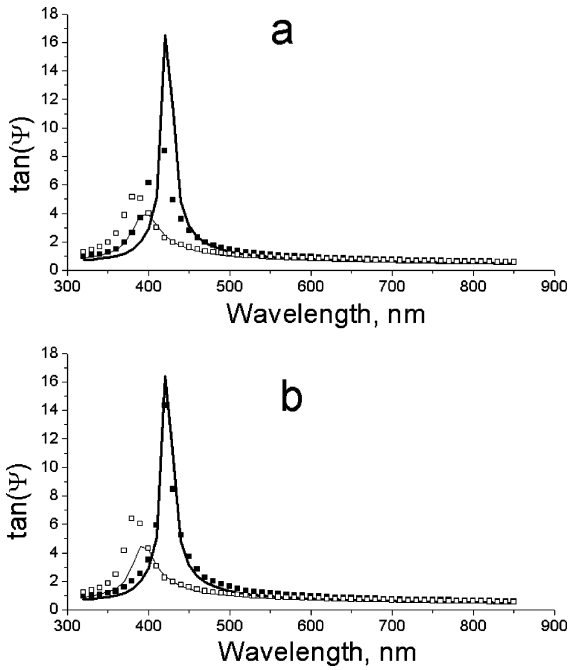

Figure 3. BSA films and corresponding porous films upon extraction with methanol as revealed by spectroscopic ellipsometry (tan(Ψ) spectra): HMeDOT (a) and ProDOT (b) BSAs. The best model fit is shown by the solid line, and the experimental data are represented by dots.

BSAs upon extraction with methanol. Concurrently, we performed a scratch test by AFM and found that the thickness of the films revealed only minor change (within 3% difference). This was evidence for the formation of porous films of the neat BCP. Using the Maxwell−Garnett effective media approximation

$$\frac{\varepsilon_{eff} - \varepsilon_2}{\varepsilon_{eff} + 2\varepsilon_2} = \varphi_1\left(\frac{\varepsilon_{eff} - \varepsilon_1}{\varepsilon_{eff} + 2\varepsilon_1}\right) \quad (1)$$

where ε_{eff}, ε_1, and ε_2 are effective dielectric constant and dielectric constant of phase 1 and phase 2, respectively, and φ_1 is the volume fraction of phase 1; we performed estimation of the porosity and compared them with the results of the calculations based on the amounts of the additive in the BSAs. The BSAs of HMeDOT and ProDOT contain 15.3 and 13.8 mass % of additives, respectively. Assuming the density of the P4VP-additive associate to be 1 g/cm^3, the porosity of the films resulting from methanol extraction is to be the same. Ellipsometry reveals significant porosity values in both films: 14.8% and 12.6% for HMeDOT and ProDOT BSA films of about 80 nm in thickness, respectively.

Atomic Force Microscopy. The morphology of thin films of the compositions provides important information about the BSA formation. This is due to the phenomenon of microphase separation in BSAs similarly to neat BCPs.[1] The morphology depends on Flory's immiscibility of the polymer blocks and the volume ratio of the blocks constituting the BCP. In the case of BSA, its morphology can change qualitatively compared to the parent BCP. This is due to the increasing volume fraction of one of the blocks if a selective interaction of the additive takes place (Figure 4). In particular, we have observed formation of

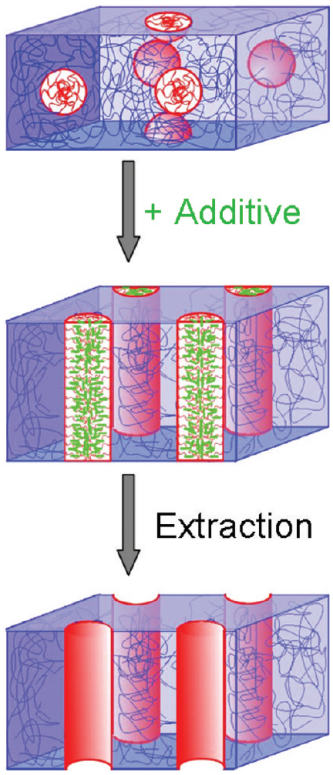

Figure 4. Concept of the morphology changes upon formation of BSA: spherical bcc morphology of the parent BCP (top) undergoes transformation to cylinders upon formation of the assembly with an additive. Successive extraction of the additive with a selective solvent results in porous film (bottom).

BSA of PS-P4VP + HABA[10] with AFM supported by other methods. The parent BCP with about 10% volume fraction of

dx.doi.org/10.1021/ma2011798 | *Macromolecules* 2012, 45, 275−282

P4VP revealed spherical bcc morphology. Selective interaction with a bulky additive HABA resulted in increase of the fraction of P4VP + HABA up to 25%. The cylindrical morphology is characteristic for such volume fraction of minor component; this has been proven by the extensive AFM studies.[9,10] Here we compare the morphology of thin films of two compositions, i.e., PS-P4VP + HMeDOT and PS-P4VP + ProDOT, with parent PS-P4VP. The AFM images of thin films of the parent BCP reveal spherical bcc morphology with the periodicity of 23 nm; the representative images of the height and phase signals along with the FFT and the power spectrum density plot of the parent BCP film are shown in the Supporting Information.

Thin films of BSA of HMeDOT deposited from its solution in 1,4-dioxane are microscopically smooth with rms roughness of 0.5 nm on a 1 × 1 μm^2 scale. However, the phase signal in tapping mode resolves the surface pattern of quasi-hexagonally ordered features. FFT conversion of the phase image clearly reveals the periodicity of 28.5 ± 1.0 nm. (Both images and the power spectrum density plot of the composition are provided in the Supporting Information.) Subsequent extraction of HMeDOT by methanol reveals quasi-hexagonal order of nanoscopic wells (Figure 5a) with the periodicity of 28.5 ± 1.0 nm. Apparently, being a selective solvent, methanol dissolves HMeDOT, leaving PS matrix of the BSA film unaffected. Similarly to the HABA-based BSA, vapor annealing in 1,4-dioxane improves the ordering (Figure 5b). The insets show FFT images of HMeDOT BSA films "as is" and upon vapor annealing. The FFT image in Figure 5a ("as is") reveals a halo corresponding to the periodicity of 28.5 nm. The FFT image of the BSA film upon vapor annealing demonstrates six sharp first-order peaks corresponding to the periodicity of 32.0 nm and the higher-order peaks spaced at $\sqrt{3}$ of main peak revealing the hexagonal order.

The hexagonal pattern of the film surface observed by AFM can reflect either spherical bcc morphology or perpendicular cylinders of P4VP + HMeDOT. Assuming the latter case, we have performed vapor annealing of the BSA film in chloroform. Indeed, AFM demonstrates the fingerprint-like pattern. Some regions with mixed orientation are also seen revealing incomplete switching of the orientation (Figure 5c). Similarly to the HABA BSA, periodicity of the parallel oriented cylinders is higher than in perpendicular orientation and is equal to 33.8 nm. We explain this apparent discrepancy by fast drying of the swollen film, which results in a distorted hexagonal matrix.[10]

The BSA of EDOT with PS-P4VP is a challenge to characterize. From spectroscopic ellipsometry time-resolved serial measurements we have found that liquid EDOT evaporates from thin films of its BSA within 3−5 min. Its evaporation results in collapse of the polystyrene matrix, leaving the morphology almost identical to the parent BCP (Supporting Information). Therefore, it is very difficult to characterize and manipulate thin films of EDOT BSA. However, we succeeded in AFM imaging a thin film of the BSA with EDOT. Immediately upon deposition by spin-coating, the film was immersed in methanol. Being insoluble in methanol, the morphology of the matrix was preserved and available for AFM characterization. The result is shown in Figure 6. It reveals a combination of dots and short stripes. Usually this is associated with weakly ordered cylinders of mixed orientation. The periodicity of the BSA with EDOT (~34 nm) overwhelmingly exceeds the periodicity of the parent BCP. These are the signs of the BSA formation, although the lack of direct evidence is apparent. Therefore, we have chosen a solid-state analogue of EDOT, i.e., ProDOT, as a model compound to investigate non-HB BSAs based on thiophenes and pyridines.

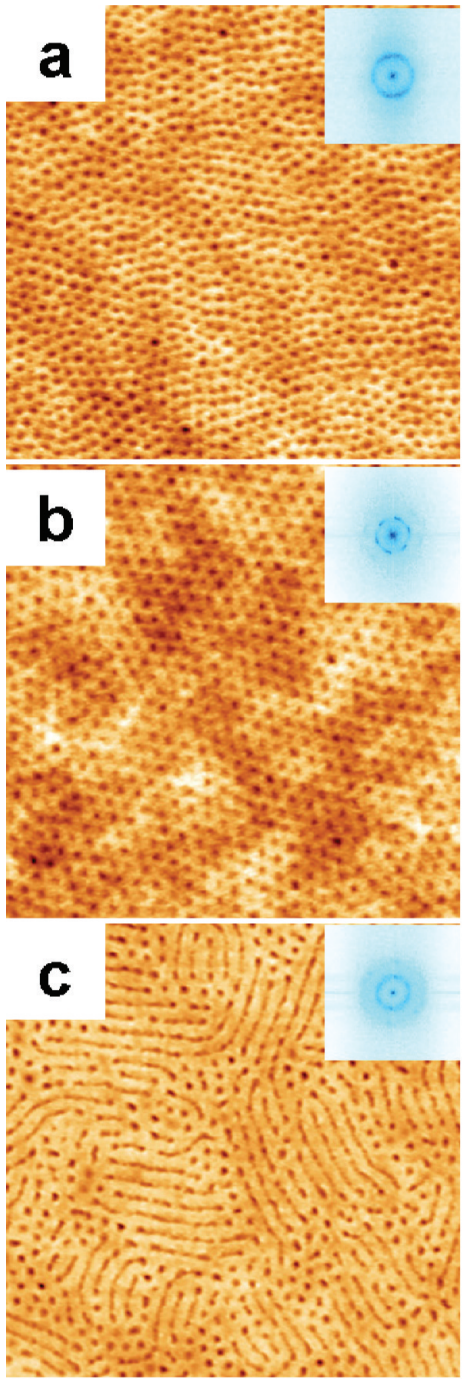

Figure 5. AFM images (topography) of thin films of HMeDOT BSA upon deposition (a), vapor annealing in 1,4-dioxane (b), and vapor annealing in chloroform (c). All images are 1 × 1 μm^2 scan size. The additive is extracted by methanol to reveal the structure. Insets: corresponding FFT images.

The BSA of ProDOT with PS-P4VP demonstrates good ability to form thin films with no signs of ProDOT macrophase separation (crystallization). This is the first indication of the formation of the BSA. The AFM image of ProDOT BSA reveals mixed morphology (Figure 7). We found that thinner films (30−50 nm in thickness) demonstrate preferentially hexagonal patterns with only a few elongated features (Figure 7a). The surface of the thicker films (50−80 nm in thickness) is

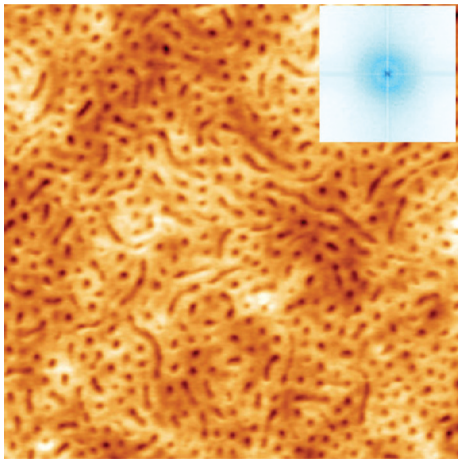

Figure 6. AFM image (topography) of thin films of EDOT BSA, 1 × 1 μm^2 scan size. The additive is extracted by methanol instantly upon deposition to preserve the structure and to reveal the features. Inset: corresponding FFT image.

dominated by elongated features (parallel cylinders) with a small number of dots (Figure 7b). Although the classical fingerprint-like morphology is absent, the presence of elongated features clearly indicates cylindrical morphology of the BSA in mixed orientation. The comparison of the periodicity observed in thin films of the parent BCP (23 nm, Supporting Information) and the films of the BSA with ProDOT (29−34 nm, Figure 7c) is further evidence for the BSA formation. Compared to the spherical morphology of the BCP, it clearly shows preferential interaction of ProDOT with the block of P4VP. Apparently, it can result in an increase of the volume fraction of the minor phase (P4VP) in the BCP from 0.110 up to 0.254 in the BSA, taking into account the equimolar composition (ProDOT vs P4VP) and assuming density of both blocks about 1 g/cm^3.

The fingerprint-like pattern would clearly indicate the formation of cylindrical morphology of parallel orientation. Formerly, we have used vapor annealing to switch the orientation of the BSA with HABA. Depending on selectivity of the solvent used for vapor annealing, either perpendicular (hexagonal pattern, 1,4-dioxane) or parallel (fingerprint-like, chloroform) orientations have been documented. Therefore, we applied a similar procedure to the BSA with ProDOT. However, vapor annealing in chloroform resulted in separation of ProDOT from the film in the form of crystals. AFM analysis of the surface revealed the morphology identical to the parent BCP. The rinse with methanol led to no changes in the surface morphology. Similar results were observed for vapors of 1,4-dioxane and THF. We concluded therefore that vapors of polar solvents have a destructive effect on the ProDOT interactions with the pyridines as they can replace the molecules of the additive in the BSA with non-HB interactions.

EDOT and its analogues are well-known as precursors for intrinsically conducting polymers (ICP). We have succeeded in oxidative polymerization of ProDOT *in situ* in the template of its BSA. In order to realize it, we have altered the approach of oxidative chemical vapor deposition designed by Gleason[46] to thin films of ProDOT BSA. We exposed the BSA films to I_2 vapors at room temperature overnight. The samples were then placed in a vacuum oven at 60 °C for 1 h to remove excess I_2. Because of higher optical density of poly(ProDOT), the films revealed more dense color though the thickness remained the same before and after polymerization as measured by the AFM

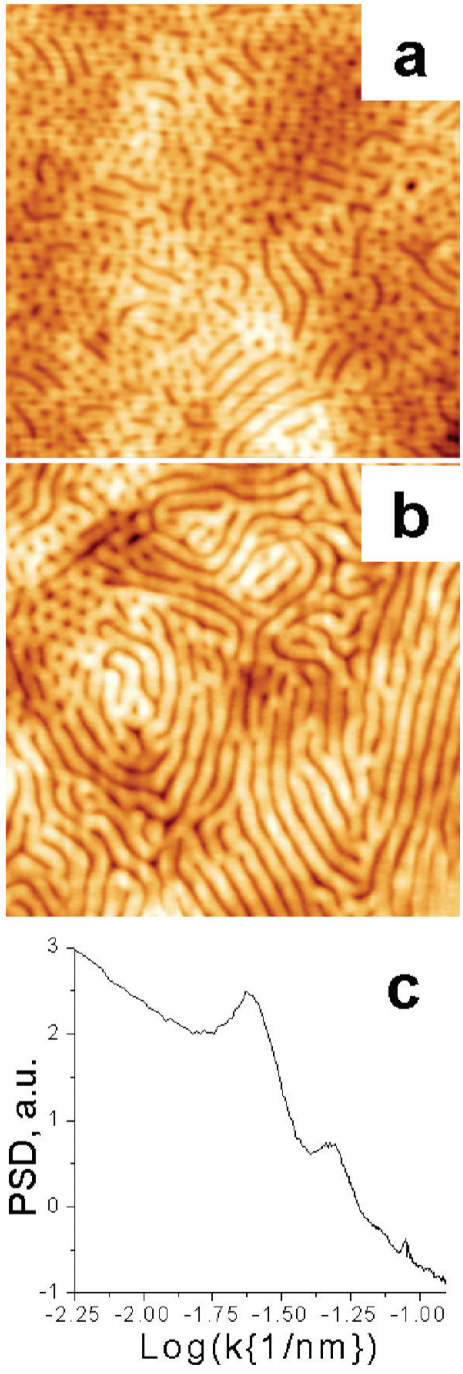

Figure 7. AFM image (topography) of thin films of ProDOT BSA revealing diversity of the patterns: majority of dots (thickness 50 nm, a) and majority of stripes (thickness 70 nm, b). 1 × 1 μm^2 scan size. A representative power spectrum density plot (c) reveals typical periodicity of ∼32 nm. The additive is extracted by methanol to reveal the structure.

scratch test. Selective plasma etching allowed us to reveal the composition as shown in Figure 8a. The features protruding through the film surface are the columns of the poly(ProDOT) while the PS matrix is partially etched away. The remaining films are insoluble in good solvents as a result of partial cross-linking of PS matrix and strong entanglement of poly(ProDOT) domains with chains of P4VP. Such films demonstrate modest conductivity as was revealed by a conductive AFM (Figure 8b).

dx.doi.org/10.1021/ma2011798 | *Macromolecules* 2012, 45, 275−282

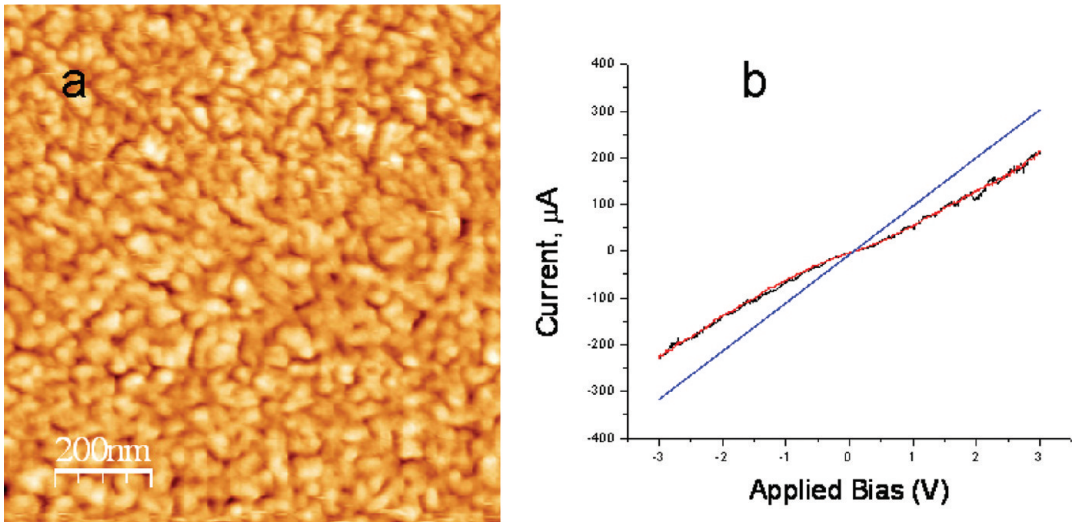

Figure 8. AFM image (topography) of partially etched sample with ProDOT BSA upon oxidative polymerization, 1 × 1 μm^2 scan size (a). Conductivity scan (C-AFM) between 3 and −3 V, forward (black) and backward (red); shunt 10 kohm resistor in the circuit. Blue line: reference scan of bare gold film (b).

DISCUSSION

The results presented above clearly indicate the fact of formation of a non-HB BSA. There are two important questions to be discussed. First, how does the energy of non-HB interactions between an additive and the units of BCP affect the stability and behavior of the BSA? Second, what is the nature of the interactions we observe in the BSA of PS-P4VP + ProDOT?

The first sign of the formation of the ProDOT was the change in the periodicity of the hexagonal pattern compared to the neat BCP of PS−PVP. Indeed, increase of the periodicity from 23 nm (parent BCP) to ∼30 nm (BSA) is quite substantial. Is the change in the periodicity enough to unambiguously conclude that the BSA is formed, though? It is probably true for relatively strong interactions, for instance when hydrogen bonds are formed: the preferential interactions of the components of the HABA and PDP BSAs are obvious from their molecular structures. However, in the case of non-HB interactions, the selectivity becomes an important factor, and concurrent interactions can play an important role. In particular, increased periodicity observed in the case of PS−P4VP + ProDOT (Figure 9a) can be explained by either (i) nonselective incorporation of molecules of the additive into both domains of the BCP, or (ii) preferential interaction with the major component (matrix), or (iii) preferential interaction with the minor component to an extent that the cylindrical morphology is achieved. In the two former cases the morphology is bcc spheres, and AFM would reveal hexagonally ordered dots. In the latter case either hexagonal arrays of dots (perpendicular orientation) or fingerprint-like patterns (parallel to surface orientation) are to be observed. Also, parallel oriented cylinders are usually associated with terraces; their height is commensurable with the cylinders' size. The formation of terraces allows one to distinguish between parallel oriented cylinders and perpendicular lamellae.

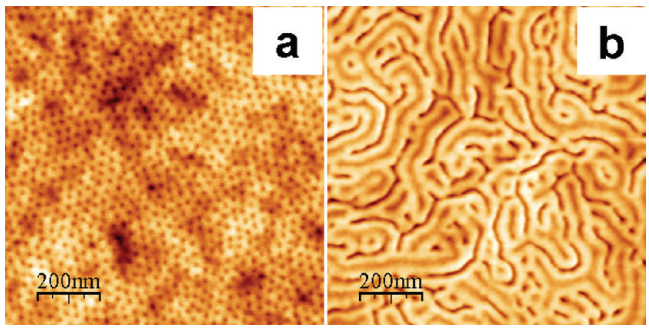

Figure 9. Vapor annealing of ProDOT BSA films in benzyl alcohol results in surface reconstruction from perpendicular cylinders (a) to parallel cylinders (b).

This reasoning led us to find conditions when both parallel and perpendicular orientations of cylinders can be observed using the AFM. This situation was observed for ProDOT BSA (Figure 7a,b) when, depending on the thickness, either preferentially perpendicular or preferentially parallel cylinders were observed. However, the switching of the orientation seemed to be the most unequivocal proof of the cylindrical morphology and thus selective interaction of the additive with P4VP block of the BCP. Our efforts to find the condition of orientation control of the BSA with ProDOT together with reasoning about the fine balance of polar and nonpolar interactions with the different components of the BSA resulted in such compound. The annealing of the BSA films in vapors of benzyl alcohol resulted in well-developed stripe patterns typical for parallel cylinders[47] (Figure 9b). Noteworthy, the starting morphology was perpendicular cylinders (hexagonal, Figure 9a). No signs of the destruction of the BSA (crystals, dewetting) were observed.

The second question relates to the nature of the interactions and requires consideration of possible interactions on the molecular level. As two model compounds we use EDOT and 4-ethylpyridine (4EP). The results of the partial charge distribution (Mulliken charges) calculated using DFT with basis set B3LYP/6-31G (open shell) are shown in Figure 10. First, they clearly indicate the possibility of strong Coulomb interactions between the positively charged sulfur of EDOT (+0.41) and the negatively charged nitrogen of pyridine ring (−0.37). Assuming head-to-head alignment of the donor (EDOT) and acceptor (4EP) and a distance between sites of 0.3 nm, we obtain the energy of Coulomb interaction about 10 kT for PS as media

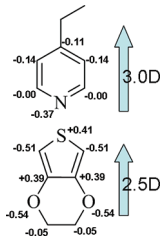

Figure 10. Two model compounds used for molecular simulation: 4-ethylpyridine (top) and EDOT (bottom). Results of DFT (B3LYP/6-31G) calculations in terms of Mulliken partial charges.

(ε = 2.6):

$$w(r) = -\frac{Q_S Q_N}{4\pi\varepsilon_0 \varepsilon r} \quad (2)$$

Second, both molecules have a substantial dipole moment of 2.98 D (4-ethylpyridine) and 2.47 D (EDOT). Using the Keesom equation for angle-averaged dipole−dipole interaction[48]

$$w(r) = -\frac{u_{EDOT}^{2} u_{4EP}^{2}}{3(4\pi\varepsilon_0)^2 kTr^6} \quad (3)$$

we obtain 230 kT for vacuum at r = 0.3 nm. Taking into account the dielectric constant of PS of 2.6, the energy value decreases to 34 kT. Therefore, both the Coulomb attraction between donor and acceptor sites and the dipole−dipole Keesom interaction seem to be substantial for stable non-HB BSA at room temperature.

Apparently, further analysis of the molecular interactions is required; both experimental aspects and high-level molecular simulations are expected to provide more details on the BSA formation. This work is ongoing, and the results will be reported elsewhere.

CONCLUSION

In this paper we report three new BSAs based on PS−P4VP and low molecular weight additives of the EDOT family: EDOT, ProDOT, and HMeDOT. The latter additive selectively interacts with pyridine rings of the P4VP block through the formation of hydrogen bonds. Conversely, the other two additives form BSAs in spite of the fact that they are not capable of hydrogen bonding with P4VP. Further comparison of HB and non-HB BSAs shows that non-HB BSAs are less stable. However, they can produce thin films with cylindrical morphology. The orientation of the cylinders can be switched by annealing in vapors of a suitable solvent. Extraction of the additive by a selective solvent (methanol) results in porous films. This allowed us to investigate their morphology by AFM and spectroscopic ellipsometry. On the other hand, gas phase oxidative polymerization *in situ* in the BSA template results in conductive polymer domains distributed in the matrix of parent polymer. Further studies on the nature of the interactions and manipulations are ongoing.

EXPERIMENTAL SECTION

Materials. Polystyrene-*block*-poly(4-vinylpyridine) (PS−P4VP), with the molecular masses (M_n) of PS 35 500 g mol^{-1}, P4VP 4400 g mol^{-1}, M_w/M_n = 1.09 for both blocks, and poly(4-vinylpyridine) with M_n 3200 g mol^{-1}, M_w/M_n = 1.20 were purchased from Polymer Source, Inc. 3,4-Ethylenedioxythiophene (EDOT), hydroxymethyl EDOT (HMeDOT), and 3,4-(2,2-dimethylpropylenedioxy)thiophene (ProDOT) were purchased from Sigma-Aldrich. Solvents chloroform, dichloromethane, 1,4-dioxane, benzyl alcohol, and methanol were purchased from Sigma-Aldrich and used as supplied. Silicon wafers {100} were cleaned successively in an ultrasonic bath (dichloromethane, methanol, Millipore water) for 15 min each and then in 2:1:1 alkali "piranha" solution (H_2O:H_2O_2:NH_4OH) at 82 °C for 40 min. The wafers were then rinsed thoroughly with Millipore water and dried by blowing with an argon stream.

Instrumentation. A Thermo Nicolet Avatar 370 spectrometer was used to collect the FTIR spectra. The spectra were taken using an ATR Smart Performer accessory (Ge crystal) from 4000 to 400 cm^{-1} at 1 or 4 cm^{-1} resolution and 32 or 64 scans.

Atomic force microscopy (AFM) images were obtained using a Veeco diInnova scanning probe microscope in tapping mode. The AFM probes (Budget Sensors) used have the following features: resonant frequency of 160−180 kHz and spring constant of about 48 N/m. The AFM images were treated (linear flattening) and analyzed using WsXM software (Nanotec Electronica).[49] Conductive AFM probing was done using CONTPt probes (NanoWorld, Inc.) on samples deposited on 100 nm thick film of Au. The sample holder was equipped with 10 kohm resistor (shunt) to prevent circuit shortage.

Psi and Delta profiles were obtained using a PHE-102 spectroscopic ellipsometer (Angstrom Advanced Inc.). Measurements were per formed at an incident angle of 70° in the wavelength range 320−850 nm.

Sample Preparation. The equimolar BSAs of PS−P4VP and the additives (with respect to P4VP units) were used throughout. The parent BCP and the additive were dissolved separately in 1,4-dioxane. The BCP solution was then added dropwise to the additive solution while it was kept in an ultrasonic bath and being mildly heated (40 °C). The BSA solution containing HMeDOT was aged at least 48 h prior to thin film deposition. The solutions of EDOT and ProDOT were aged at least 1 week prior to deposition to establish equilibrium and complete BSA formation.

Ellipsometry and AFM measurements were done on thin films deposited from the BSA solutions. They were deposited by either dip-coating or spin-coating techniques. Dip-coating was used to produce films between 30 and 60 nm. Spin-coating was used to deposit thicker films, 60−120 nm. Before depositions, all solutions were filtered using 0.2 μm PTFE filters.

Annealing in vapors of 1,4-dioxane, chloroform, and benzyl alcohol: the samples were exposed to the solvent vapor so that film thickness increased ~3 times. This was estimated by the color (interference) of the film. They were left in the swollen state for about 30 min and then immediately removed from the chamber.

ASSOCIATED CONTENT

Supporting Information

AFM images of thin films of neat (parent) BCP (Figure S1) and HMeDOT BSA as deposited (no extraction) (Figure S3) as reference materials; details for FTIR spectra of P4VP−HMEDOT associate (Figure S2). This material is available free of charge via the Internet at http://pubs.acs.org.

AUTHOR INFORMATION

Corresponding Author

*Tel (215) 596 8836; e-mail a.sidorenko@usp.edu.

ACKNOWLEDGMENTS

This work was funded by National Science Foundation (DMR 0947897) and in part by the Center for Drug Design and Delivery (KISK grant of the Department of Community and Economic Development, Commonwealth of Pennsylvania). The authors acknowledge helpful discussions with Dr. J. D. Tovar, Johns Hopkins University, Dr. V. Pophristic, University of the Sciences, Dr. I. Tokarev, and Prof. S. S. Minko, Clarkson University. T. P. Enright acknowledges financial support of his fellowship at NIST (SURF Award).

REFERENCES

(1) Bates, F. S.; Fredrickson, G. H. *Annu. Rev. Phys. Chem.* **1990**, *41*, 525−557.
(2) Muthukumar, M.; Ober, C. K.; Thomas, E. L. *Science* **1997**, *277*, 1225−1232.
(3) Matsen, M. W.; Bates, F. S. *Macromolecules* **1996**, *29*, 1091−1098.
(4) Ruokolainen, J.; Makinen, R.; Torkkeli, M.; Makela, T.; Serimaa, R.; ten Brinke, G.; Ikkala, O. *Science* **1998**, *280*, 557−560.
(5) Ruokolainen, J.; ten Brinke, G.; Ikkala, O.; Torkkeli, M.; Serimaa, R. *Macromolecules* **1996**, *29* (10), 3409−3415.
(6) Bondzic, S.; De Wit, J.; Polushkin, E.; Schouten, A. J.; Ten Brinke, G.; Ruokolainen, J.; Ikkala, O.; Dolbnya, I.; Bras, W. *Macromolecules* **2004**, *37* (25), 9517−9524.
(7) Polushkin, E.; Bondzic, S.; de Wit, J.; van Ekenstein, G. A.; Dolbnya, I.; Bras, W.; Ikkala, O.; ten Brinke, G. *Macromolecules* **2005**, *38* (5), 1804−1813.
(8) Laforgue, A.; Bazuin, C. G.; Prud'homme, R. E. *Macromolecules* **2006**, *39* (19), 6473−6482.
(9) Sidorenko, A.; Tokarev, I.; Minko, S.; Stamm, M. *J. Am. Chem. Soc.* **2003**, *125* (40), 12211−12216.
(10) Tokarev, I.; Krenek, R.; Burkov, Y.; Schmeisser, D.; Sidorenko, A.; Minko, S.; Stamm, M. *Macromolecules* **2005**, *38* (2), 507−516.
(11) Ali, N.; Park, S.-Y. *Langmuir* **2009**, *25* (23), 13426−13431.
(12) Kuila, B. K.; Gowd, E. B.; Stamm, M. *Macromolecules* **2010**, *43* (18), 7713−7721.
(13) Rancatore, B. J.; Mauldin, C. E.; Tung, S.-H.; Wang, C.; Hexemer, A.; Strzalka, J.; Frechet, J. M. J.; Xu, T. *ACS Nano* **2010**, *4* (5), 2721−2729.
(14) Tata, J.; Scalarone, D.; Lazzari, M.; Chiantore, O. *Eur. Polym. J.* **2009**, *45* (9), 2520−2528.
(15) Rodriguez, A. T.; Li, X.; Wang, J.; Steen, W. A.; Fan, H. *Adv. Funct. Mater.* **2007**, *17* (15), 2710−2716.
(16) Lee, J.-W.; Lee, C.-S.; Choi, S.-Y.; Kim, S.-H. *Macromolecules* **2010**, *43* (1), 442−447.
(17) Tenneti, K. K.; Chen, X.; Li, C. Y.; Wan, X.; Fan, X.; Zhou, Q.-F.; Rong, L.; Hsiao, B. S. *Macromolecules* **2007**, *40* (14), 5095−510.
(18) du Sart, G. G.; Vukovic, I.; Vukovic, Z.; Polushkin, E.; Hiekkataipale, P.; Ruokolainen, J.; Loos, K.; ten Brinke, G. *Macromol. Rapid Commun.* **2011**, *32* (4), 366−370.
(19) Leolukman, M.; Paoprasert, P.; Mandel, I.; Diaz, S. J.; McGee, D. J.; Gopalan, P. *J. Polym. Sci., Part A: Polym. Chem.* **2009**, *47* (19), 5017−5026.
(20) Jeong, U.; Kim, H. C.; Rodriguez, R. L.; Tsai, I. Y.; Stafford, C. M.; Kim, J. K.; Hawker, C. J.; Russell, T. P. *Adv. Mater.* **2002**, *14*, 274−276.
(21) Ruokolainen, J.; Ten Binke, G.; Ikkala, O. *Adv. Mater.* **1999**, *11* (9), 777−780.
(22) Sun, Z.; Bai, F.; Wu, H.; Schmitt, S. K.; Boye, D. M.; Fan, H. *J. Am. Chem. Soc.* **2009**, *131* (38), 13594−13595.
(23) Seifarth, O.; Schmeisser, D.; Krenek, R.; Sydorenko, A.; Stamm, M. *Prog. Solid State Chem.* **2006**, *34* (2−4), 111−119.
(24) Krenek, R.; Stamm, M.; Cimrova, V. *J. Appl. Phys.* **2008**, *103* (4), 044306/1−044306/16.
(25) Gowd, E. B.; Nandan, B.; Vyas, M. K.; Bigall, N. C.; Eychmueller, A.; Schloerb, H.; Stamm, M. *Nanotechnology* **2009**, *20* (41), 415302/1−415302/10.
(26) Kuila, B. K.; Stamm, M. *J. Mater. Chem.* **2010**, *20* (29), 6086−6094.
(27) Schwark, D.; Vezie, D.; Reffner, J.; Annis, B.; Thomas, E. *J. Mater. Sci. Lett.* **1992**, *11*, 352−355.
(28) van Zoelen, W.; Polushkin, E.; ten Brinke, G. *Macromolecules* **2008**, *41* (22), 8807−8814.
(29) Zettl, U.; Knoll, A.; Tsarkova, L. *Langmuir* **2010**, *26* (9), 6610−6617.
(30) Kriksin, Y. A.; Khalatur, P. G.; Erukhimovich, I. Ya.; ten Brinke, G.; Khokhlov, A. R. *Soft Matter* **2009**, *5* (15), 2896−2904. van Zoelen, W.; ten Brinke, G. *Soft Matter* **2009**, *5* (8), 1568−1582.
(31) Supramolecular materials based on hydrogen-bonded polymers: ten Brinke, G.; Ruokolainen, J.; Ikkala, O. *Adv. Polym. Sci.* **2007**, *207*, 113−177.
(32) Ligthart, G. B. W. L.; Scherman, O. A.; Sijbesma, R. P.; Meijer, E. W. *Macromol. Eng.* **2007**, *1*, 351−399.
(33) Heywang, G.; Jonas, F. *Adv. Mater.* **1992**, *4* (2), 116−18.
(34) Sun, J.; Zhang, B.; Katz, H. E. *Adv. Funct. Mater.* **2011**, *21* (1), 29−45.
(35) Roncali, J. *Electrochem. Commun.* **2000**, *2*, 72−76.
(36) Stephan, O.; Schottland, P.; Le Gall, P.-Y.; Chevrot, C.; Mariet, C.; Carrier, M. *J. Electroanal. Chem.* **1998**, *443* (2), 217−22.
(37) Kim, S.; Taya, M. *Electrochim. Acta* **2010**, *55* (19), 5307−5311.
(38) Welsh, D. M.; Kumar, A.; Meijer, E. W.; Reynolds, J. R. *Adv. Mater.* **1999**, *11* (16), 1379−1382.
(39) Coleman, M. M.; Graf, J. F.; Painter, P. C. *Specific Interactions and the Miscibility of Polymer Blends*; Technomic: Lancaster, PA, 1991.
(40) Cesteros, L. C.; Meaurio, E.; Katime, I. *Macromolecules* **1993**, *26*, 2323.
(41) Cesteros, L. C.; Isasi, J. R.; Katime, I. *Macromolecules* **1993**, *26*, 7256.
(42) Cesteros, L. C.; Jose', L.; Katime, I. *Polymer* **1995**, *36*, 3183.
(43) Takahashi, H.; Mamola, K.; Plyler, E. K. *J. Mol. Spectrosc.* **1966**, *21*, 217.
(44) Plate, N. A.; Shibaev, V. P. *Comb-Shaped Polymers and Liquid Crystals*; Plenum Press: New York, 1987.
(45) Ruokolainen, J.; Torkkeli, M.; Serimaa, R.; Vahvaselkae, S.; Saariaho, M.; ten Brinke, G.; Ikkala, O. *Macromolecules* **1996**, *29* (20), 6621−6628.
(46) Lock, J. P.; Im, S. G.; Gleason, K. K. *Macromolecules* **2006**, *39* (16), 5326−5329.
(47) Hamley, I. W. Introduction to Block Copolymers. In *Developments in Block Copolymer Science and Technology*; Hamley, I. W., Ed.; John Wiley & Sons: New York, 2004.
(48) Israelachvili, J. *Intermolecular and Surface Forces*, 2nd ed.; Academic Press: New York, 1991; pp 57−63.
(49) Horcas, I.; Fernandez, R.; Gomez-Rodriguez, J. M.; Colchero, J.; Gomez-Herrero, J.; Baro, A. M. *Rev. Sci. Instrum.* **2007**, *78*, 013705.